

Article

Experimental Tests and Reliability Analysis of the Cracking Impact Resistance of UHPFRC

Hussain A. Jabir ¹, Sallal R. Abid ¹, Gunasekaran Murali ², Sajjad H. Ali ¹, Sergey Klyuev ³, Roman Fediuk ^{4,*}, Nikolai Vatin ⁵, Vladimir Promakhov ⁶ and Yuriy Vasilev ⁷

¹ Civil Engineering Department, Wasit University, Kut 52001, Iraq; haskar@uowasit.edu.iq (H.A.J.); sallal@uowasit.edu.iq (S.R.A.); sajad_alzuhery@yahoo.com (S.H.A.)

² School of Civil Engineering, SASTRA Deemed to be University, Thanjavur 613401, India; murali@civil.sastra.edu

³ Department of Theoretical Mechanics and Strength of Materials, Belgorod State Technological University Named after V.G. Shukhov, 308012 Belgorod, Russia; Klyuyev@yandex.ru

⁴ Polytechnic Institute, Far Eastern Federal University, 690922 Vladivostok, Russia

⁵ Higher School of Industrial, Civil and Road Construction, Peter the Great St. Petersburg Polytechnic University, 195251 St. Petersburg, Russia; vatin@mail.ru

⁶ Additive Technology Center, National Research Tomsk State University, 634050 Tomsk, Russia; vvpromakhov@mail.ru

⁷ Department of Road-Building Materials, Moscow Automobile and Road Construction University, 125319 Moscow, Russia; yu.vasilev@madi.ru

* Correspondence: roman44@yandex.ru

Received: 9 November 2020; Accepted: 2 December 2020; Published: 4 December 2020



Abstract: Ultra-high performance (UHP) concrete is a special type of fibrous cementitious composite that is characterized by high strength and superior ductility, toughness, and durability. This research aimed to investigate the resistance of ultra-high performance fiber-reinforced concrete (UHPFRC) against repeated impacts. An adjusted repeated drop mass impact test was adopted to evaluate the impact performance of 72 UHPFRC disc specimens. The specimens were divided into six mixtures each of 12 discs. The only difference between the mixtures was the types of fibers used, while all other mixture components were the same. Three types of fibers were used: 6 mm micro-steel, 15 mm micro-steel, and polypropylene. All mixtures included 2.5% volumetric content of fibers, however with different combinations of the three fiber types. The test results showed that the mixtures with the 15 mm micro-steel fiber absorbed a higher number of impact blows until cracking compared to other mixtures. The mixture with pure 2.5% of 15 mm micro-steel fiber exhibited the highest impact resistance, with percentage increases over the other mixtures ranging from 25 to 140%. In addition, the Weibull distribution was used to investigate the cracking impact resistance of UHP at different levels of reliability.

Keywords: impact test; repeated drop-weight; ACI 544-2R; UHPFRC; Weibull distribution

1. Introduction

The strength of any reinforced concrete structural member relies on its cross-sectional geometry, span between supports, amount and distribution of reinforcement, in addition to the concrete material's properties. The strength of concrete is a key material property that controls the design under any type of loading. Among the possible applied loads is the impact load, which can be a design load, as in the case of airport runways, where impact loads are generated by the wheels of the landing aircrafts. Similarly, offshore structures are designed to absorb repeated impacts from sea waves [1–5], while the impacts from waterborne materials on the horizontal and vertical surfaces of stilling basin parts in

hydraulic structures is another example of design impact loads [6,7]. However, other structures that are typically not designed to withstand repeated impact loads may also be subjected to accidental impacts arising from falling masses from higher altitudes, vehicle collisions, or projectiles during wars or terrorist acts [8–11]. Therefore, it is becoming more important with time to consider the impact resistance seriously, either through proper design or by using sufficient concrete materials.

Normal concrete is known for its low impact resistance, while fibrous concretes have been proven to withstand higher impact loads before failure. Concrete reinforced by steel or synthetic fibers, such as polypropylene fibers, were tested under different load conditions and different loading types. Such materials were found to have superior flexural strength, tensile strength, shear strength, ductility, and toughness compared to normal concrete of the same compressive strength design [12–15]. On the other hand, previous studies have shown that the impact resistance values of concretes reinforced with steel or synthetic fibers are far superior to normal concrete [16–20].

Several recent researchers have focused on the hybridization of metallic and synthetic fibers to achieve better performance and loading and higher durability. The term “hybrid-fiber-reinforced concrete” refers to concrete that includes more than one type of fiber or different shapes or sizes of the same type of fiber. Due to their high modulus of elasticity and strength, which increase the initial strength of the concrete, steel fibers are the most used fiber type, coming in several different shapes (straight, hooked-end, and crimped) and sizes, while polymer fibers such as polypropylene (PP), polyvinyl alcohol (PVA), or others are used to improve durability, shear strength, ductility, and flexural performance [21–24]. Qian and Stroeven [25] used combinations of the three types of steel fibers and PP fibers to evaluate the influence of hybrid fiber reinforcement on concrete mechanical properties. The used steel fibers were 6 mm long straight fibers and 30 and 40 mm long hooked-end fibers. The results showed that the strength improvement induced by hybrid fibers can be similar to that attained by using the largest amount of monofibers. Yao et al. [26] used a low amount (0.5%) of steel and PP fibers both separately and as a hybrid combination. They recorded better mechanical performance for hybrid fibers compared to monofibers, with the best performance being observed for the mixture containing 30% volume of PP and 70% volume of steel fibers. Aiming to enhance the ductility of light-weight concrete, Libre et al. [27] investigated hybrid combinations of steel and PP fibers. They revealed that adding 0.4% of PP fiber to the hybrid fibrous mixture improved the ductility. This result was confirmed by other researchers [28], who showed better flexural performance, higher toughness, and improved compressive strength and splitting tensile strength for hybrid fibrous high-strength concrete. Rashiddadash et al. [29] investigated four volumetric combinations of steel and PP fibers at a total volume content of 1.0%. The test results showed that increasing the volume percentage of steel fibers and decreasing the percentage of PP fibers resulted in better mechanical properties and flexural toughness. On the other hand, other researchers [30] showed better flexural toughness for mixtures incorporated with both PP and steel fibers.

Previous experimental studies were carried out to understand the impact performance of hybrid-fiber-reinforced concrete [31–38]. Several metallic and synthetic or natural fibers were incorporated into different types of concretes and cementitious composites. The projectile impact test was the focus of some previous studies [31–34], while others investigated the flexural impact of hybrid fibrous concrete [35,36]. However, few studies were found in the literature on repeated low-velocity drop impacts on hybrid fibrous concrete incorporated with steel and PP fibers. Yildirim et al. [37] tested 12 normal-strength concrete mixtures containing steel fibers, steel-PP hybrid fibers and steel-glass hybrid fibers using a similar procedure to that of the ACI 544-2R [38] repeated drop mass impact test. The steel fiber content varied from 0.5 to 1.0%, while only 0.1% of PP or glass fibers was used. The results revealed that steel fibers provided greater improvements in impact resistance compared to PP and glass fibers, and that steel-PP hybrid fibers showed potential resistance to cracking induced by repeated impacts. Naraganti et al. [39] conducted repeated impact tests following the ACI 544-2R [38] method on normal-strength fibrous concrete incorporating mono-steel, PP, or sisal fibers, in addition to hybrid steel-PP and steel-sisal fibers. Their test results revealed that sisal fibers exhibited the lowest impact

resistance, while steel fibers exhibited the highest impact resistance among the monofibrous mixtures. The test results also showed that the best performance and highest impact resistance among all mixtures were recorded for hybrid steel–PP fibers. Ali et al. [40] used the ACI 544-2R [38] repeated drop mass impact test to study the impact behavior of engineered cementitious composites reinforced with hybrid PVA and short-metal alloy (SMA) fibers. The tests were conducted before and after heating to 150 °C. The test results showed that mono and hybrid fibers increased the impact resistance by 30 to 100 times compared to the plain mixtures. It was also concluded that the highest impact performance was recorded for the mixture containing 2% PVA and 1% SMA.

UHPFRC concrete is a type of modern fibrous concrete that has considerably high strength and superior durability properties [41,42]. Extensive research studies are available in the literature on the compressive [43], tensile, flexural, and shear strengths of UHPFRC under different exposure conditions. However, the available literature on the impact behavior of UHPFRC using the different impact tests is limited [44]. Moreover, those that were conducted using the repeated drop mass impact test were very limited [45,46]. Feng et al. conducted repeated drop mass impact tests on UHPFRC mixtures containing mono and hybrid fibers. Sixteen UHP mixtures were prepared and tested using steel, PVA, and PP fibers, with volumetric contents ranging from 1.5 to 2.5%. The test results showed that for the same volumetric contents, both PVA and PP fibers (when added to steel fibers) improved the impact failure resistance compared to monofibrous mixtures. When combined with steel fibers, PVA showed the potential for increased cracking resistance, which increased as the PVA content increased. On the other hand, for the same total volume content, the increased PP content in hybrid steel–PP mixtures resulted in lower impact resistance.

The presented literature review clearly revealed that the behavior of hybrid fibrous high-performance concrete HPC under repeated drop mass has barely been investigated, with a very limited number of studies available. To enrich the available knowledge on the research area, the impact properties of UHPFRCs reinforced with mono-steel, hybrid steel, and hybrid steel–PP fibers were investigated experimentally. This research was sequentially conducted as follows: (1) Impact samples were prepared from UHP mixtures containing six different hybrid combinations of steel and PP fibers. (2) Impact tests were performed based on the repeated impact testing technique described in ACI 544-2R. (3) The results were statically analyzed using the Weibull distribution. Such research is required due to the lack of sufficient research studies on the impact properties of hybrid-fiber-reinforced UHPFRCs.

2. Materials and Methods

Metallic and synthetic fibers were used in this study to evaluate the influence of the inclusion of hybrid fibers on the impact resistance of UHPFRC. Different combinations of the three types of fibers were utilized in six mixtures. Excluding fiber types and dosages, all other constituents were identical in the six mixtures. Hence, the same quantities of dry materials, water, and admixtures were used in the six mixtures. Two types of micro-steel fibers were utilized in this research: 6 mm long micro-steel fibers (S6) and 15 mm long micro-steel fibers (S15). In addition to the micro-steel fibers, polypropylene fibers (PP) were used in three of the six mixtures. Figure 1 shows pictures of the used micro-steel and polypropylene fibers and the cast impact specimens, while Table 1 shows details of the six UHPFRC mixtures. The total volumetric content of the fibers was kept constant for all six mixtures at 2.5%. In the first mixture (M1), only 6 mm micro-steel fiber (S6) was used, while in the second mixture (M2) only S15 micro-steel fiber was used. The 2.5% fiber volumetric content of the third mixture (M3) was split equally between S6 and S15 fibers at 1.25% each, as shown in Table 1. The fourth mixture (M4) contained a hybrid fiber combination of S6 micro-steel fibers and polypropylene fibers, at 2.0 and 0.5% volumetric contents, respectively. Similarly, the fifth mixture (M5) included 2.0% of the S15 micro-steel fiber and 0.5% of the PP fiber. Finally, the sixth mixture (M6) included all three fiber types, with volumetric contents for S6, S15, and PP of 1.0, 1.0, and 0.5%, respectively.

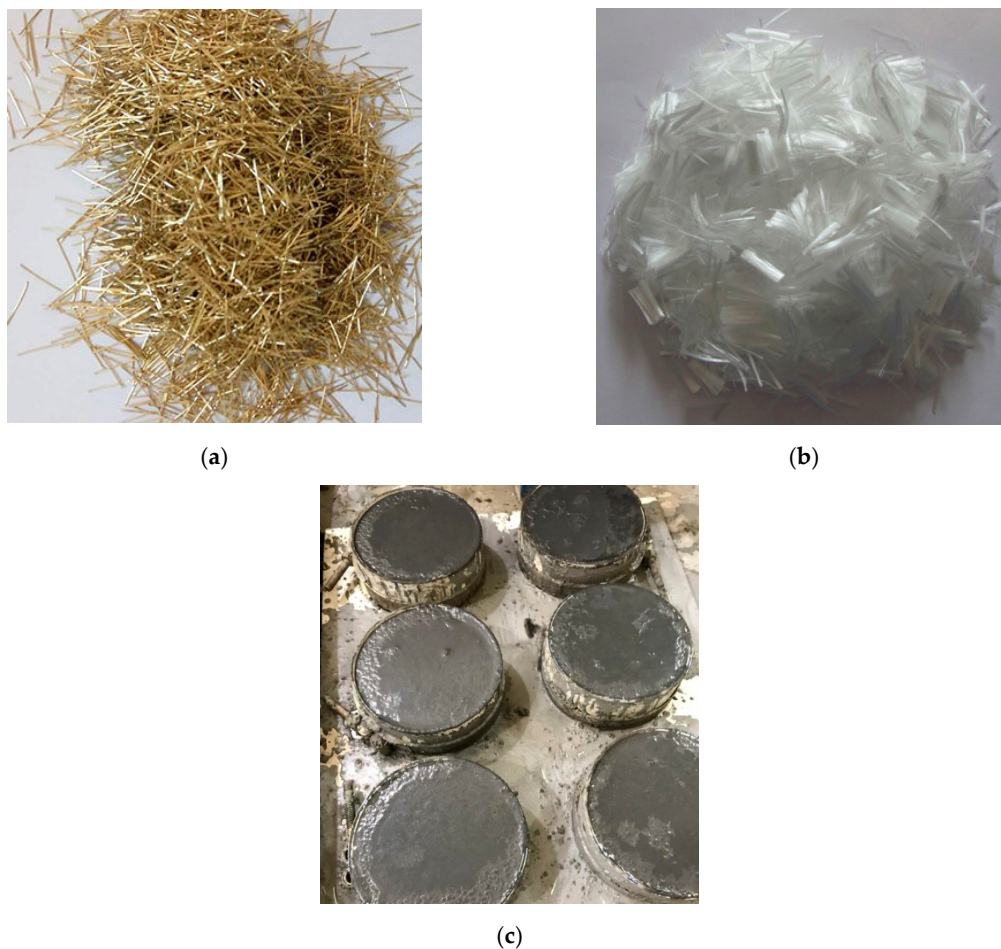


Figure 1. The used (a) micro-steel fibers, (b) polypropylene fibers, and (c) the cast disc specimens.

Table 1. Mix proportions of the six ultra-high performance fiber-reinforced concrete(UHPFRC) mixtures.

Material	M1	M2	M3	M4	M5	M6
Cement (kg/m ³)	800	800	800	800	800	800
Silica Fume (kg/m ³)	240	240	240	240	240	240
Fly Ash (kg/m ³)	120	120	120	120	120	120
Silica Sand (kg/m ³)	960	960	960	960	960	960
Water (kg/m ³)	232	232	232	232	232	232
SP (kg/m ³)	47	47	47	47	47	47
S6 fiber (V _f %)	2.5	0	1.25	2.0	0	1.0
S15 fiber (V _f %)	0	2.5	1.25	0	2.0	1.0
PP fiber (V _f %)	0	0	0	0.5	0.5	0.5

Ordinary Portland cement type 42.5 was the main cementitious material in all mixtures, with a specific gravity of 3.15 and a specific surface area of 362 m²/kg. In addition to cement, silica fume was used as an additional cementitious material, which has a specific gravity of 2.2 and a specific surface area of 21,000 m²/kg. Fly ash with a specific gravity of 2.2 was also used in all mixtures in this study, as shown in Table 1. Fine silica sand with grain sizes ranging from 0.08 to 0.2 mm was used as the only filler in the mixtures. The dry bulk density of the used silica sand was 1500 kg/m³. Sika ViscoCrete-5930 superplasticizer (SP) was utilized in the six mixtures to achieve the required workability. The diameters of the used steel fibers (S6 and S15) were 0.12 and 0.2 mm, respectively, while their aspect ratios were 50 and 75, respectively. The density of both fibers was 7800 kg/m³, while their ultimate tensile strengths were 2.85 and 2.6 GPa, respectively. On the other hand, the length, diameter, and aspect ratio of the PP

fibers were 18 mm, 0.5 mm, and 36, respectively, while the density and ultimate tensile strength of the PP fibers were 910 kg/m^3 and 0.35 GPa, respectively.

The impact and control tests were conducted at an age of 28 days. All specimens were kept in temperature-controlled water tanks until the testing date. To conduct the repeated impact test, the average of twelve discs was adopted. Thus, a total of 72 impact disc specimens were tested in this study. To evaluate the quality of the concrete, both compressive strength and splitting tensile strength tests were conducted. Six cubes of 150 mm side length were used to evaluate the compressive strength of each mixture, while six cylinders with 100 mm diameter and 200 mm length were cast and tested to evaluate the splitting tensile strength. Thus, in total, 36 cubes and 36 cylinders were cast and tested in this study, in addition to the impact discs.

Figure 2 shows the details of the repeated drop mass impact (RDMI) technique used in this study, which follows the recommendations of ACI 544-2R [38]. Among several tests that have been used during the last few decades to evaluate the impact performance of concrete, the RDMI test is considered as the simplest and most economical one. This test relies on the registration of the required number of drop impact blows to initiate the surface cracking of the target specimen and to cause its failure by splitting into several parts. Hence, no sophisticated load, velocity, displacement, or strain sensors and no data measurement and collection systems are required. The whole process is mechanical and manual, whereby a specific steel mass of approximately 4.5 kg is lifted vertically along two smooth steel shafts (to reduce the friction) to the specified height of approximately 450 mm. After resting at the design altitude, the mass is released to freely fall onto the target specimen. This process is conducted repeatedly until cracking and ultimately until failure of the target specimen. The standard target specimen is a concrete disc that has a diameter and depth of approximately 150 and 63 mm, respectively. To allow for better stress distribution, the impact load is transferred to the test target via a steel ball with a diameter of approximately 63 mm. The steel ball is left to rest before testing on the top surface of the target specimen using a holding frame, as shown in Figure 2. To assure that no rebound movements occur, the target specimen is tightened using four steel lugs and elastomers. After recording the number of impacts that caused cracking, the elastomers are removed and the impact test is continued until the specimen touches at least three of the four steel lugs, which means that the cracks have been opened wide enough to consider this as target failure.

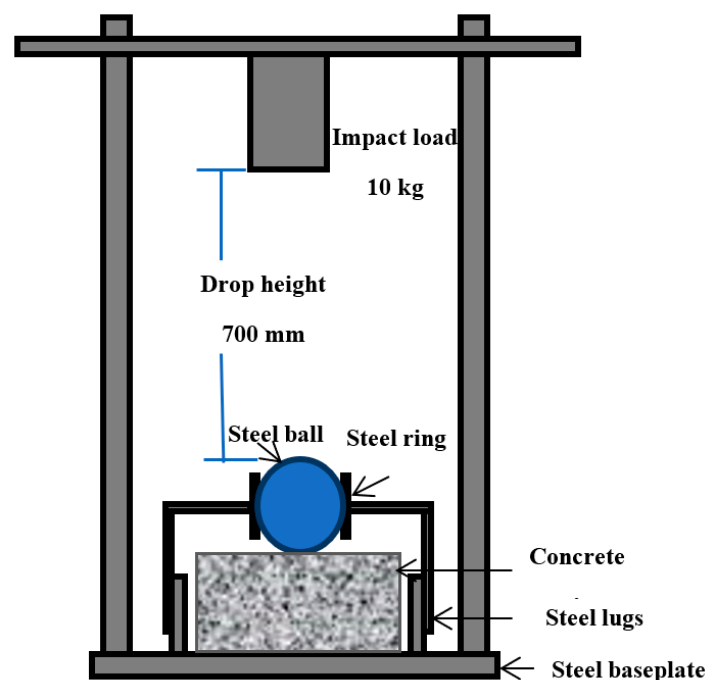


Figure 2. Details of the repeated drop mass impact (RDMI)_ testing apparatus.

In this research, and as shown in Figures 2 and 3, the above technique was used, but with a higher impact height of 700 mm and a higher impact mass of 10 kg. Both the impact mass and height were increased to maximize the impact force of each blow, and thus to reduce the efforts required to crack the target specimen. The resulting impact force from each blow was approximately 3.5 times that of the standard mass and height of ACI 544-2R. Hence, the number of blows was reduced significantly, reducing the total labor effort required. This modification was conducted because of the expected high impact resistance of the used UHPFRC, which is attributed to the high contents of cementitious materials and fibers. Moreover, and considering the same purpose, the diameter of the target disc specimens used in this study was 125 mm, which is 25 mm less than that of the standard ACI 544-2R, while the disc depth was 65 mm.

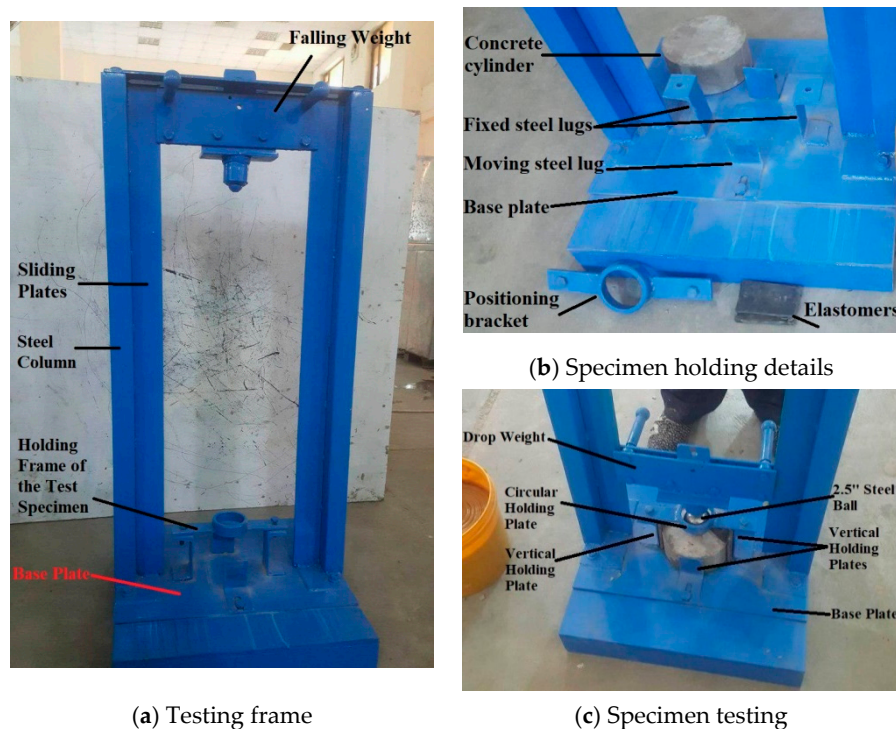


Figure 3. The used RDMI testing apparatus.

3. Results

The results of the material control tests, including compressive strength and splitting tensile strength results, are listed in Table 2. The table shows the compressive strength results for two ages of 7 and 28 days, while the splitting tensile strength was tested at the age of 28 days only. The test results show that the yielded compressive strengths at both ages were not significantly different between the different groups. However, it is obvious that mixes with micro-steel fibers only had higher compressive strengths than the hybrid ones containing micro-steel and polypropylene fibers, which can be attributed to the high stiffness of steel fibers compared to PP fibers. Comparing M1 with M4, it is obvious that the 28 day compressive strength of M1 was higher than that of M4 by 6.0%. Similarly, the compressive strength of M2 was higher than that of M5 by 3.4%, while M3 was higher than M6 by 3.6%. As noted, the percentage differences between the two groups of mixtures (without and with PP fiber) were between 3.4 and 6.0%, which are relatively small differences to be considered as a trend.

It is also noted that the mixture with pure 6 mm micro-steel fiber (M1) retained higher compressive strength than that with pure 15 mm micro-steel fiber (M2), while the maximum compressive strength was retained when the two fibers were mixed equally, as in mixture M3. Similar results can be observed for groups M4 to M6 with PP fibers, where M4 retained higher 28 day compressive strength

than M5, while the maximum among this group was for M6, containing mixed 6 mm and 15 mm micro-steel fibers.

Table 2. Compressive strength and splitting tensile strength test results.

Mixture	Compressive Strength (MPa)		Splitting Tensile Strength (MPa)
	7 Days	28 Days	
M1	56.6	81.5	10.58
M2	48.7	77.74	13.18
M3	58.7	82.8	10.71
M4	45.3	76.9	10.28
M5	47.5	75.2	14.03
M6	48.6	79.6	11.45
SD	5.41	2.88	1.545
COV	10.63	3.65	13.2

Table 3 shows the results of the repeated impact tests for the specimens of the six UHPFRC mixtures. Each point represents the average of 12 disc specimens. It should be noted here that the impact tests were not continued until failure for all specimens because of their very high number of impacts required to induce failure, which required extensive efforts and a very long testing time. Considering the manual operation of the testing apparatus as per the recommendations of ACI 544-2R, and although the impact force increased with each impact blow, the determination of the number of impacts causing failure can delay the testing schedule, which may affect the reliability of the test results, as some specimens would be tested at older ages. Therefore, the material behavior under repeated impact testing was analyzed based on target cracking only.

Table 3. Number of impacts taken to cause cracking for the six UHPFRC mixtures.

Specimen No	M1	M2	M3	M4	M5	M6
1	33	102	53	60	60	54
2	71	140	60	78	127	63
3	91	172	89	85	146	65
4	114	189	90	89	156	72
5	115	210	93	110	175	77
6	130	243	97	117	190	80
7	133	251	110	121	206	90
8	135	267	122	121	228	94
9	150	286	135	122	233	101
10	172	293	135	132	250	136
11	182	302	144	154	276	198
12	201	490	216	233	318	201
Mean	127	245	112	118	197	102
SD	47.4	99.5	43.5	44.4	70.4	50.1
COV	37.27	40.55	38.81	37.49	35.72	48.81

It is obvious that the inclusion of the 15 mm micro-steel fibers had a greater effect on the impact resistance compared to the 6 mm micro-steel fibers and PP fibers. Considering the first group of mixtures without PP fibers (M1, M2, and M3), M2 (pure 15 mm micro-steel fiber) resisted a higher number of impacts compared to the other groups. The number of impacts that caused cracking for M2 (pure 15 mm micro-steel fiber) was 245 blows, while those of M1 and M3 were 127 and 112, respectively. Similarly, among the second group of mixtures, where 0.5% of PP was used in conjunction with 2.0% of steel fibers, the number of impacts that caused cracking for mixture M5 (2.0% of 15 mm micro-steel fiber) was 197. On the other hand, the numbers of impacts that caused cracking for mixtures M4 and M6 were 118 and 102, respectively. This behavior can firstly be attributed to the higher stiffness and

surface hardness of steel fibers compared to PP fibers, and secondly to the larger shielded concrete area behind the 15 mm micro-steel fibers owing to their length compared to the 6 mm ones, which delayed the surface fractures, and hence crack initiation.

4. Weibull Distribution

Several studies have been carried out to predict the composite failure [47,48]. Wallodi Weibull initially developed the Weibull distribution, which is utilized for many engineering applications. The Weibull distribution function is characterized by shape and scale parameters; these parameters play a crucial part in reliability analysis. As a result of repetition from previous studies, the two Weibull parameter distributions have been proven to be the more suitable, approved, and suggested distribution functions for measuring the impact resistance of concrete [47–49]. In line with ACI Committee 544, drop weight experimental findings are not reliable at a minimum of three samples per mix, an outcome that was found by earlier researchers [47,48]. Huge variations in test results were reported in many studies, the reason for which can be ascribed to the following causes [18,47,48]: (i) crack initiation must be found by visual surveillance, which can happen in any direction; (ii) the results of the drop weight test are attained by means of impact strikes at one location on the concrete’s surface, possibly on a hardened substance containing coarse aggregate or on the smooth interlayer of the cement matrix; (iii) fiber-reinforced concretes are heterogeneous materials, which can cause variance in the mix design, resulting in impact energy variations; (iv) the tests depend on the 4.5 kg drop weight being lifted and dropped at the same point in time at a height of 450 mm, which is a very difficult job. Considering the abovementioned points, it can be concluded that a reliable statistical tool is needed to analyze the variations in test results, which would be a suitable remedy for the differences in drop weight impact results. Differences in the experimentally tested results can be predicted by a function of the two-parameter Weibull distribution—the density probability function is articulated in Equation (1) [50]:

$$f(N_f) = \frac{b}{Z_a - N_0} \left[\frac{Z_f - Z_0}{Z_a - Z_0} \right]^{b-1} \exp \left\{ - \left[\frac{Z_f - Z_0}{Z_a - Z_0} \right]^b \right\} (Z_0 \leq Z_f < \infty) \tag{1}$$

where *b* is the shape parameter, *Z_a* is a scale parameter of the impact strength, and *Z₀* is the impact strength safety at the minimum level. The impact strength (number of blows) *Z_f* is a variable in the Weibull distribution. The impact strength under the survival possibility *P* is defined as *Z*. By deriving Equation (1), the distribution function *F(Z)* is obtained and is expressed in Equation (2) [50]:

$$F(Z_p) = P(Z_f < Z_p) = 1 - \exp \left\{ - \left[\frac{Z_p - Z_0}{Z_a - Z_0} \right]^b \right\} \tag{2}$$

Here, the probability of failure is *P* (*Z_f* < *Z*). Then:

$$P(Z_f > Z_p) = 1 - P(Z_f < Z_p) = \exp \left\{ - \left[\frac{Z_p - Z_0}{Z_a - Z} \right]^b \right\} \tag{3}$$

From Equation (3), if *b*, *Z_a*, and *Z₀* are all known within a specific rate of survival *P*, it helps to obtain *Z*. Since the impact strength of concrete is distinct, the *Z₀* values of normal and fibrous concrete are taken as 0 [47]. Therefore, Equation (1) can be simplified into the two-parameter Weibull function as follows:

$$f(Z_f) = \frac{b}{N_a} \left[\frac{Z_f}{Z_a} \right]^{b-1} \exp \left\{ - \left[\frac{Z_f}{Z_a} \right]^b \right\} (Z_0 \leq Z_f < \infty) \tag{4}$$

The possibility of survival P and the failure probability can be expressed as:

$$p = \exp\left\{-\left[\frac{Z_f}{Z_a}\right]^b\right\} \tag{5}$$

$$p' = 1 - p == 1 - \exp\left\{-\left[\frac{Z_f}{Z_a}\right]^b\right\} \tag{6}$$

Considering a natural logarithm of two sides of Equation (5), the equation obtained can be as follows:

$$\ln\left[\ln\left(\frac{1}{p}\right)\right] = b\ln Z_f - b\ln Z_a \tag{7}$$

When rearranging Equation (7) as a linear equation, we define $Y = \ln\left[\ln\left(\frac{1}{p}\right)\right] = \ln\left[\ln\left(\frac{1}{p'}\right)\right]$, $X = \ln Z_f$, $a = b\ln Z_a$. Equation (7) can be expressed as follows:

$$Y = bX - a \tag{8}$$

The above Equation (8) provides an impact strength (number of blows) defined by two Weibull parameters. The linear function of Equation (8) can be functionalized to scrutinize whether impact test data follow the two-parameter Weibull distribution. A simple linear regression analysis was performed on the impact results. If a best linear correlation is obtained between Y and X, this shows that the test data conform to the two-parameter Weibull distribution. The relationship between Z_f and p is determined from Equation (9) as follows [47]:

$$p = 1 - \frac{i}{k + 1} \tag{9}$$

where i denotes a specimen number of increased order and k denotes the total number of impact test data points. A graph is plotted between $\ln[\ln(1/p)]$ for every impact strength (number of blows) value and the corresponding impact strength of $\ln(\text{number of blows})$, as illustrated in Figures 4 and 5. If data points are correlated linearly, it can be assumed that impact strength data follow the two-parameter Weibull distribution. The shape parameter is obtained directly from the slope of the line from the linear equation, while the scale parameter is calculated from Equation (10):

$$Z_a = e^{(-a/b)} \tag{10}$$

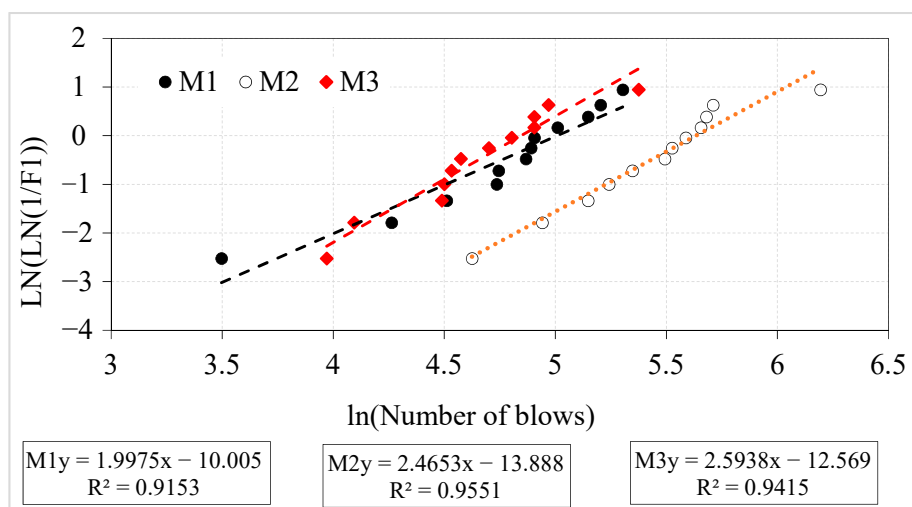


Figure 4. Weibull lines for mixes M1, M2, and M3.

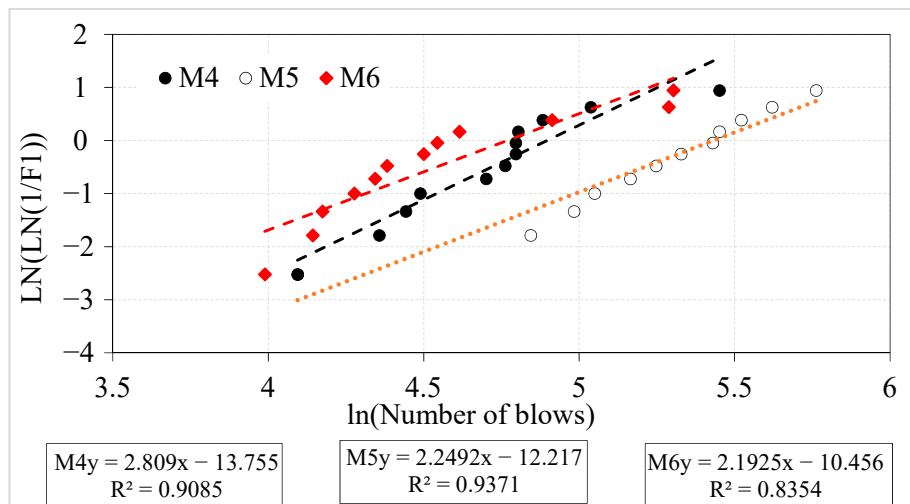


Figure 5. Weibull lines for mixes M4, M5, and M6.

The obtained scale and shape parameters are used to evaluate the impact strength (number of blows) corresponding to the predefined reliability level, which can be expressed in Equation (11) [51,52]:

$$Z_{1,2} = Z_a(-\ln(R_x))^{(1/b)} \tag{11}$$

Table 4 displays the obtained shape and scale parameters from the linear regression results for all tested specimen. It can be seen in Table 4 that the data for the Weibull distribution follow an approximated linear distribution. Furthermore, the coefficients of determination (R^2) for the fitting results for all test data are greater than 0.8 and near to 1.0. This shows that X and Y are linearly dependent. Stated differently, the impact strength (number of blows) values conform to the two-parameter Weibull distribution.

Table 4. Computed Weibull parameters.

Mix Id	b	Intercept	Z _a	R ²
M1	1.998	-10.005	150	0.9153
M2	2.465	-13.888	280	0.9551
M3	2.594	-12.569	127	0.9415
M4	2.809	-13.755	134	0.9085
M5	2.249	-12.217	229	0.9371
M6	2.193	-10.456	118	0.8354

Table 5 demonstrates the calculated impact strength (number of blows) from the reliability analysis. Considering the 0.99 reliability level, the number of blows needed to produce the initial cracks in M1, M2, M3, M4, M5, and M6 were equal to or greater than 15, 43, 22, 26, 30, and 14, respectively. Likewise, considering the 0.8 reliability level, the number of blows needed to produce the initial cracks were 71, 152, 71, 78, 117, and 59 for specimens M1, M2, M3, M4, M5, and M6, respectively. The coefficients of determination for all mixtures were higher than 0.8, revealing adequate reliability. Reliability analysis through the Weibull distribution was used to examine the variations in experimental test data. This eradicated the expenses and time needed to assess the impact strength for the tested specimens via the drop weight impact test. The impact strength can be evaluated from the proposed reliability table at the required reliability level.

Table 5. Impact strength (number of blows) values corresponding to the defined reliability levels.

Reliability Level	M1	M2	M3	M4	M5	M6
0.99	15	43	22	26	30	14
0.9	49	112	53	60	84	42
0.80	71	152	71	78	117	59
0.70	89	184	85	93	145	74
0.6	107	213	98	105	170	87
0.50	125	241	110	117	194	100
0.40	143	270	123	130	220	113
0.3	164	301	137	143	248	128
0.20	190	339	153	159	282	146
0.1	227	392	175	180	331	172
0.01	322	519	229	231	451	236

5. Conclusions

The main conclusions of the current research can be summarized as follows:

1. The differences between the compressive strength values for the six groups of specimens were in the range of 3.4 to 6.0%, meaning that the different effects of the different fiber combinations cannot be judged very well. On the other hand, the mixtures with high contents of 15 mm micro-steel fibers exhibited higher splitting tensile strength than others, showing 23 to 36% higher values. The highest splitting tensile strength value was obtained for the M5 mixture, containing 2.0% of 15 mm micro-steel fibers and 0.5% of polypropylene fibers;
2. The highest impact strength value was recorded for mixture M2, containing 2.5% of 15 mm micro-steel fibers, while the second highest was recorded for mixture M5, containing 2.0% of 15 mm micro-steel fibers and 0.5% of polypropylene fibers. The impact values for mixtures M2 and M5 were higher than those for the other mixtures by up to 140%;
3. Based on the results of the reliability analysis, by considering a level of reliability of 0.9, the computed impact strength values (number of blows) were 15, 43, 22, 26, 30, and 14 for specimens M1, M2, M3, M4, M5, and M6, respectively. Therefore, the two-parameter Weibull distribution eliminates the costly and time-consuming process required to conduct the experimental tests and enables structural design engineers to select the appropriate impact strength required for the design calculation from the developed reliability–impact strength table;
4. Some types of fibers have a significant modulus of elasticity, which is a key parameter involved in improving the strength and ductility. However, the bond and anchorage characteristics of fibers can also influence the crack number, crack width, and crack depth values, which dominate the fracture characteristics. Therefore, it is suggested that further works are required to evaluate the hybrid combinations of PP fibers with different steel fiber configurations and sizes. For instance, longer hooked-end steel fibers can be used with straight micro-steel and PP fibers.

Author Contributions: Conceptualization, S.R.A.; methodology, H.A.J., S.R.A., V.P., and S.H.A.; software, G.M.; validation, G.M., H.A.J., S.K., and R.F.; resources, S.R.A., S.H.A., S.K., and R.F.; writing—original draft preparation, S.R.A., R.F., and S.K., N.V., and G.M.; writing—review and editing, Y.V., H.A.J., N.V., and S.R.A.; visualization, S.R.A., V.P., N.V., and G.M.; supervision, S.R.A. All authors have read and agreed to the published version of the manuscript.

Funding: Funding for open access charge: Peter the Great St. Petersburg Polytechnic University, Russian Academic Excellence Project “5-100”.

Acknowledgments: The authors would like to express their gratitude to the Civil Engineering Department of Wasit University, where the experimental work was conducted.

Conflicts of Interest: The authors declare no conflict of interest.

References

1. Pan, Y.; Wu, C.; Cheng, X.; Li, V.C.; He, L. Impact fatigue behaviour of GFRP mesh reinforced engineered cementitious composites for runway pavement. *Constr. Build. Mater.* **2020**, *230*, 116898. [[CrossRef](#)]
2. Abid, S.R.; Abdul-Hussein, M.L.; Ali, S.H.; Kazem, A.F. Suggested modified testing techniques to the ACI 544-R repeated drop-weight impact test. *Constr. Build. Mater.* **2020**, *244*, 118321. [[CrossRef](#)]
3. Nili, M.; Afroughsabet, V. Combined effect of silica fume and steel fibers on the impact resistance and mechanical properties of concrete. *Int. J. Impact Eng.* **2010**, *37*, 879–886. [[CrossRef](#)]
4. Zhang, W.; Chen, S.; Zhang, N.; Zhou, Y. Low-velocity flexural impact response of steel fiber reinforced concrete subjected to freeze-thaw cycles in NaCl solution. *Constr. Build. Mater.* **2015**, *101*, 522–526. [[CrossRef](#)]
5. Wang, W.; Chou, N. The behavior of coconut fibre reinforced concrete (CFRC) under impact loading. *Constr. Build. Mater.* **2017**, *134*, 452–461. [[CrossRef](#)]
6. Abid, S.R.; Shamkhi, M.S.; Mahdi, N.S.; Daek, Y.H. Hydro-abrasive resistance of engineered cementitious composites with PP and PVA fibers. *Constr. Build. Mater.* **2018**, *187*, 168–177. [[CrossRef](#)]
7. Abid, S.R.; Hilo, A.; Ayoob, N.S.; Daek, Y.H. Underwater abrasion of steel fiber-reinforced self-compacting concrete. *Case Stud. Constr. Mater.* **2019**, *11*, e00299. [[CrossRef](#)]
8. Murali, G.; Ramprasad, K. A feasibility of enhancing the impact strength of novel layered two stage fibrous concrete slabs. *Eng. Struct.* **2019**, *175*, 41–49. [[CrossRef](#)]
9. Zhang, W.; Chen, S.; Liu, Y. Effect of weight and drop height of hammer on the flexural impact performance of fiber-reinforced concrete. *Constr. Build. Mater.* **2017**, *140*, 31–35. [[CrossRef](#)]
10. Abid, S.R.; Abdul-Hussein, M.L.; Ayoob, N.S.; Ali, S.H.; Kadhum, A.L. Repeated drop-weight impact tests on self-compacting concrete reinforced with micro-steel fiber. *Heliyon* **2020**, *6*, 1–11. [[CrossRef](#)] [[PubMed](#)]
11. Yoo, D.-Y.; Banthia, N. Impact resistance of fiber-reinforced concrete—A review. *Cem. Conc. Compos.* **2019**, *104*, 103389. [[CrossRef](#)]
12. Abbass, A.; Abid, S.; Özakça, M. Experimental investigation on the effect of steel fibers on the flexural behavior and ductility of high-strength concrete hollow beams. *Adv. Civil. Eng.* **2019**, *2019*, 1–13. [[CrossRef](#)]
13. Bošnjak, J.; Sharma, A.; Grauf, K. Mechanical Properties of Concrete with Steel and Polypropylene Fibres at Elevated Temperatures. *Fibers* **2019**, *7*, 9. [[CrossRef](#)]
14. Ghoneim, M.; Yehia, A.; Yehia, S.; Abuzaid, W. Shear Strength of Fiber Reinforced Recycled Aggregate Concrete. *Materials* **2020**, *13*, 4183. [[CrossRef](#)]
15. Abbass, A.A.; Abid, S.R.; Arna'ot, F.H.; Al-Ameri, R.A.; Özakça, M. Flexural response of hollow high strength concrete beams considering different size reductions. *Structure* **2019**, *23*, 69–86. [[CrossRef](#)]
16. Nia, A.A.; Hedayatian, M.; Nili, M.; Afroughsabet, V. An experimental and numerical study on how steel and polypropylene fibers affect the impact resistance in fiber-reinforced concrete. *Int. J. Impact Eng.* **2012**, *46*, 62–73.
17. Ismail, M.K.; Hassan, A.A.A.; Lachemi, M. Performance of self-consolidating engineered cementitious composite under drop-weight impact loading. *ASCE J. Mater. Civil. Eng.* **2019**, *31*, 1–11. [[CrossRef](#)]
18. Mastali, M.; Dalvand, A. The impact resistance and mechanical properties of self-compacting concrete reinforced with recycled CFRP pieces. *Compos. B Eng.* **2016**, *92*, 360–376. [[CrossRef](#)]
19. Ismail, M.K.; Hassan, A.A. Impact resistance and mechanical properties of self-consolidating rubberized concrete reinforced with steel fibers. *ASCE J. Mater. Civil. Eng.* **2017**, *29*, 1–14. [[CrossRef](#)]
20. Abid, S.R.; Hilo, A.; Daek, Y.H. Experimental tests on the underwater abrasion of engineered cementitious composites. *Constr. Build. Mater.* **2018**, *171*, 779–792. [[CrossRef](#)]
21. Kim, D.J.; Naaman, A.E.; El-Tawil, S. Comparative flexural behavior of four fiber reinforced cementitious composites. *Cem. Concr. Compos.* **2008**, *30*, 917–928. [[CrossRef](#)]
22. Pakravan, H.R.; Latifi, M.; Jamshidi, M. Hybrid short fiber reinforcement system in concrete: A review. *Constr. Build. Mater.* **2017**, *142*, 280–294. [[CrossRef](#)]
23. Ali, A.Y.; Al-Rammahi, A.A. Flexural Behavior of Hybrid-Reinforced Concrete Exterior Beam-Column Joints under Static and Cyclic Loads. *Fibers* **2019**, *7*, 94. [[CrossRef](#)]
24. Abdul Hussein, M.L.; Abid, S.R.; Ali, S.H. Abrasion of reactive powder concrete under water impact. *Appl. Mech. Mater.* **2020**, *897*, 41–48. [[CrossRef](#)]
25. Qian, C.X.; Stroeven, P. Development of hybrid polypropylene-steel fiber reinforced concrete. *Cem. Concr. Res.* **2000**, *30*, 63–69. [[CrossRef](#)]

26. Yao, W.; Li, J.; Wu, K. Mechanical properties of hybrid fiber-reinforced concrete at low fiber volume fraction. *Cem. Concr. Res.* **2003**, *33*, 27–30. [[CrossRef](#)]
27. Libre, N.A.; Shekarchi, M.; Mahoutian, M.; Soroushian, P. Mechanical properties of hybrid fiber reinforced lightweight aggregate concrete made with natural pumice. *Constr. Build. Mater.* **2011**, *25*, 2458–2464. [[CrossRef](#)]
28. Dawood, E.T.; Ramli, M. High strength characteristics of cement mortar reinforced with hybrid fibres. *Constr. Build. Mater.* **2011**, *25*, 2240–2247. [[CrossRef](#)]
29. Rashiddadash, P.; Ramezaniapour, A.A.; Mahdikhani, M. Experimental investigation on flexural toughness of hybrid fiber reinforced concrete (HFRC) containing metakaolin and pumice. *Constr. Build. Mater.* **2014**, *51*, 313–320. [[CrossRef](#)]
30. Kruminš, J.; Zesers, A. Experimental investigation of the fracture of hybrid fiber-reinforced concrete. *Mech. Compos. Mater.* **2015**, *51*, 25–32. [[CrossRef](#)]
31. Almusallam, T.H.; Siddiqui, N.A.; Iqbal, R.A.; Abbas, H. Response of hybrid-fiber reinforced concrete slabs to hard projectile impact. *Int. J. Impact Eng.* **2013**, *58*, 17–30. [[CrossRef](#)]
32. Fu, Q.; Niu, D.; Zhang, J.; Huang, D.; Hong, M. Impact response of concrete reinforced with hybrid basalt-polypropylene fibers. *Powder Technol.* **2018**, *326*, 411–424. [[CrossRef](#)]
33. Feng, J.; Gao, X.; Li, J.; Dong, H.; Yao, W.; Wang, X. Influence of fiber mixture on impact response of ultra-high-performance hybrid fiber reinforced cementitious composite. *Compos. Part B* **2019**, *163*, 487–496. [[CrossRef](#)]
34. Feng, J.; Gao, X.; Li, J.; Dong, H.; He, Q.; Liang, J.; Sun, W. Penetration resistance of hybrid-fiber-reinforced high-strength concrete under projectile multi-impact. *Constr. Build. Mater.* **2019**, *202*, 341–352. [[CrossRef](#)]
35. Manzhilevskaya, S.E. Organizational and economic problems of ecological safety in construction. *Constr. Mater. Prod.* **2019**, *2*, 73–78.
36. Alwesabi, E.A.; Abu Bakar, B.H.; Alshaikh, I.M.H.; Akil, H.M. Impact resistance of plain and rubberized concrete containing steel and polypropylene fiber. *Mater. Today Commun.* **2020**, *25*, 101640. [[CrossRef](#)]
37. Yildirim, S.T.; Ekinci, C.E.; Findik, F. Properties of hybrid fiber reinforced concrete under repeated impact loads. *Russian J. Nondestr. Test.* **2010**, *46*, 82–92.
38. ACI 544-2R. *Measurement of Properties of Fiber Reinforced Concrete*; American Concrete Institute ACI: Farmington Hills, MI, USA, 1999.
39. Naraganti, S.R.; Pannem, R.M.R.; Putta, J. Impact resistance of hybrid fibre reinforced concrete containing sisal fibers. *Ain Shams Eng. J.* **2019**, *10*, 297–305. [[CrossRef](#)]
40. Ali, M.A.E.M.; Soliman, A.M.; Nehdi, M.L. Hybrid-fiber reinforced engineered cementitious composite under tensile and impact loading. *Mater. Des.* **2017**, *117*, 139–149. [[CrossRef](#)]
41. Gesoglu, M.; Güneysisi, E.; Nahhab, A.H.; Yazıcı, H. Properties of ultra-high performance fiber reinforced cementitious composites made with gypsum-contaminated aggregates and cured at normal and elevated temperatures. *Constr. Build. Mater.* **2015**, *93*, 427–438. [[CrossRef](#)]
42. Roy, M.; Hollmann, C.; Wille, K. Influence of fiber volume fraction and fiber orientation on the uniaxial tensile behavior of rebar-reinforced ultra-high performance concrete. *Fibers* **2019**, *7*, 67. [[CrossRef](#)]
43. Yoo, D.-Y.; Banthia, N. Mechanical properties of ultra-high-performance fiber-reinforced concrete: A review. *Cem. Conc. Compos.* **2016**, *73*, 267–280. [[CrossRef](#)]
44. Yoo, D.-Y.; Banthia, N. Mechanical and structural behaviors of ultra-high-performance fiber-reinforced concrete subjected to impact and blast. *Constr. Build. Mater.* **2017**, *149*, 416–431. [[CrossRef](#)]
45. Feng, J.; Sun, W.; Zhai, H.; Wang, L.; Dong, H.; Wu, Q. Experimental Study on Hybrid Effect Evaluation of Fiber Reinforced Concrete Subjected to Drop Weight Impacts. *Materials* **2018**, *11*, 2563. [[CrossRef](#)] [[PubMed](#)]
46. Jabir, H.A.; Abid, S.R.; Abdul-Hussein, M.L.; Ali, S.H. Repeated drop-weight impact tests on RPC containing hybrid fibers. *Appl. Mech. Mater.* **2020**, *897*, 49–55. [[CrossRef](#)]
47. Murali, G.; Abid, S.R.; Amran, Y.H.M.; Abdelgader, H.S.; Fediuk, R.; Susrutha, R.; Poonguzhali, K. Impact performance of novel multi-layered prepacked aggregate fibrous composites under compression and bending. *Structure* **2020**, *28*, 1502–1515. [[CrossRef](#)]
48. Murali, G.; Asrani, N.P.; Ramkumar, V.R.; Siva, A.; Haridharan, M.K. Impact resistance and strength reliability of novel two-stage fibre-reinforced concrete. *Arabian. J. Sci. Eng.* **2019**, *44*, 4477–4490. [[CrossRef](#)]
49. Chen, X.L.; Zhu, X.Q. Mechanical behavior and damage evolution for concrete subjected to multiple impact loading. *KSCE J. Civil. Eng.* **2017**, *21*, 2351–2359. [[CrossRef](#)]

50. Chen, X.; Liu, Z.; Guo, S.; Huang, Y.; Xu, W. Experimental study on fatigue properties of normal and rubberized self-compacting concrete under bending. *Constr. Build. Mater.* **2019**, *205*, 10–20. [[CrossRef](#)]
51. Abirami, T.; Loganaganandan, M.; Murali, G.; Fediuk, R.; Sreekrishna, R.V.; Vignesh, T.; Januppriya, G.; Karthikeyan, K. Experimental research on impact response of novel steel fibrous concretes under falling mass impact. *Constr. Build. Mater.* **2019**, *222*, 447–457. [[CrossRef](#)]
52. Salaimanimagudam, M.P.; Suribabu, C.R.; Murali, G.; Abid, S.R. Impact response of hammerhead pier fibrous concrete beams designed with topology optimization. *Period. Polytech-Civ.* **2020**. [[CrossRef](#)]

Publisher’s Note: MDPI stays neutral with regard to jurisdictional claims in published maps and institutional affiliations.



© 2020 by the authors. Licensee MDPI, Basel, Switzerland. This article is an open access article distributed under the terms and conditions of the Creative Commons Attribution (CC BY) license (<http://creativecommons.org/licenses/by/4.0/>).